

## Turbulence wave number spectra reconstruction from radial correlation reflectometry data revisited in 2D theory

E Z Gusakov, M A Irzak, A Yu Popov, N V Teplova

*Ioffe Institute, St Petersburg, Russia*

Radial correlation reflectometry (RCR) utilizing simultaneous plasma probing by two microwave beams at slightly different frequencies incident normally onto the magnetic surface, and analysis of backscattering signals have been already used for plasma turbulence characterization in magnetic fusion devices for more than two decades. This diagnostic benefits from a relative technical simplicity, however the interpretation of experimental data is complicated by the dominant contribution of small-angle-scattering off long-scale fluctuations leading to a substantial overestimation of the turbulence correlation length.

Recently, two approaches were proposed theoretically to cope with the problem of high small-angle-scattering contribution in reflectometry experiment. The first is based on a mathematical procedure of the turbulence spectrum reconstruction from the RCR data developed in the 1D theoretical model [1, 2]. It uses the explicit expressions for the small-angle-scattering efficiency dependence on the fluctuation radial wavenumber provided by 1D theory [1] and takes a minor role of 2D effects for granted. The second approach, so called radial correlation Doppler reflectometry (RCDR), benefits directly from suppression of the small-angle scattering component in the reflectometer signal, taking place at the oblique enough incidence of the probing wave onto the magnetic surface. This approach was justified in [3] where the dependence of the sufficient incidence angle on a priori unknown turbulence correlation length was demonstrated.

In the present paper we perform analysis of RCR in the framework of 2D model and justify the reconstruction procedure proposed in [1] in the case of incidence of probing waves onto the plasma close to normal. According to [1] in the case of linear density profile the turbulence wavenumber spectrum can be obtained from the RCR cross-correlation function (CCF) dependence on probing frequencies using the Fourier transform

$$n_{\kappa}^2 \sim |\kappa| \int_{-\infty}^{+\infty} CCF(\omega_0, \omega_1) \exp(i\kappa\Delta L) d\Delta L \quad (1)$$

where  $n_{\kappa}^2$  is the radial wavenumber spectrum of density fluctuations;  $CCF(\omega_0, \omega_1) = \langle A_s(\omega_0) A_s^*(\omega_1) \rangle$  is the cross-correlation function of scattering signals  $A_s(\omega_0)$  and  $A_s(\omega_1)$  at frequencies  $\omega_0$  and  $\omega_1$  in the reference and signal channels,

respectively;  $\langle \dots \rangle$  stands for statistical averaging over an ensemble of the fluctuations;  $\Delta L = \frac{2(\omega_l - \omega_0)}{\omega_0} L_{\omega_0}$  is the radial separation of the cutoff positions for different probing frequencies;  $L_{\omega}$  is the density scale length at the frequency  $\omega$  wave cutoff surface. Expression (1) is valid in wide wavenumber domain determined by condition  $\kappa \geq L^{-1}$ . Unfortunately, as the drift wave turbulence, being strongly elongated along the magnetic field, is nevertheless actually two-dimensional, the 1D analysis resulting in (1) appears to be oversimplified, that stimulates us treating the RCR performance in slab 2D geometry.

In the 2D case the reflectometry scattering signal is provided by the reciprocity theorem in the form of an integral over the plasma cross-section perpendicular to the magnetic field

$$A_S(\omega) = i \frac{e^2 \sqrt{P}}{4m_e \omega} \int_S \tilde{n}(\vec{r}_\perp) E_a^2(\omega, \vec{r}_\perp) d\vec{r}_\perp \quad (2)$$

where  $P$  is the probing ordinary wave power over a unit length in the magnetic field direction,  $e$  and  $m_e$  are the electron charge and mass, respectively,  $\tilde{n}(\vec{r}_\perp)$  is the spatial distribution of the density fluctuations,  $E_a(\omega, \vec{r}_\perp)$  is the phase calibrated probing wave amplitude at frequency  $\omega$  corresponding to the unit power launched through the receiving antenna into the unperturbed plasma, and  $S$  is the plasma poloidal cross-section. According to (2) the cross-correlation function of two scattering signals at slightly different probing frequencies  $\omega_0$  and  $\omega_l$  is determined by a multiple integral

$$CCF(\omega_0, \omega_l) = \frac{e^4 P}{(4m_e \omega)^2} \iint_{SS'} d\vec{r}_\perp d\vec{r}'_\perp E_a^2(\omega_0, \vec{r}_\perp) E_a^2(\omega_l, \vec{r}'_\perp) \langle \tilde{n}(\vec{r}_\perp) \tilde{n}(\vec{r}'_\perp) \rangle \quad (3)$$

The probing wave electric field  $E_a$  here can be represented as a superposition of the partial waves emitted by the antenna  $E_a(\vec{r}_\perp) = \int_{-\infty}^{\infty} \frac{dk_y}{2\pi} f(k_y) \exp(ik_y y) W(x, k_y)$  with  $|f(k_y)|^2$  being the antenna directivity diagram over the poloidal wave number  $k_y$  and  $W(x, k_y)$  in the case of the linear density profile is given in terms of the integral proportional to the Airy function

$$W(x, k_y) = \sqrt{\frac{8\omega_0 \ell}{c^2}} \exp\left(i\Phi(k_y) - i\Phi\left(\frac{\omega}{c} \sin \vartheta\right) - i\frac{\pi}{4}\right) \int_{-\infty}^{\infty} \exp\left(i\frac{t^3}{3} + i\frac{x - L(k_y)}{\ell} t\right) dt \quad (4)$$

where  $\Phi(k_y) = \frac{\omega}{c} \int_0^{L(k_y)} dx \sqrt{(L(k_y) - x)/L_\omega}$ ;  $L(k_y) = L_\omega \left(1 - k_y^2 c^2 / \omega^2\right)$ ,  $\ell = (L_\omega c^2 / \omega^2)^{1/3}$  is the Airy scale and  $\vartheta$  standing for the tilting angle of the probing beam with respect to the

density gradient. In the present paper when performing numerical evaluation of the CCF using (3) we assume the Gaussian antenna diagram  $f(k_y) = (2\sqrt{\pi}\rho)^{1/2} \exp\left[-(k_y - \omega/c \cdot \sin \theta)^2 \rho^2/2\right]$  with  $2\rho$  being a probing microwave beam waist. The density fluctuation two-point CCF is also assumed Gaussian  $\langle \delta n(x, y) \delta n(x', y') \rangle = \delta n^2 \exp\left\{-[(x-x')^2 + (y-y')^2]/l_c^2\right\}$ . The results of the RCR CCF computation in the case of normal incidence ( $\theta = 0^\circ$ ) of a wide microwave beam ( $\rho = 1.6\text{cm}$ ) at frequency  $\omega/2\pi = 75\text{GHz}$  onto the “large” plasma ( $L = 12\text{cm}$ ) is shown in Fig.1. The probing wave cutoff in this case is situated in the antenna near field. The turbulence correlation length is taken to be small  $l_c = 0.4\text{cm}$ , however the corresponding RCR CCF appears to be much wider. Accordingly, the Fourier transform of the RCR CCF results in the RCR spectrum, which is substantially narrower than the turbulence radial wavenumber spectrum, as it is seen in Fig.2. However, after multiplication by the wavenumber absolute value  $|\kappa|$ , in accordance with 1D procedure based on (1), the RCR spectrum appears to be similar to the turbulence spectrum (see Fig.2). The difference at small wavenumbers is related to the extrapolation of CCF dependence at large  $\Delta L$  in Fig.1 when making the Fourier transform. Then the inverse Fourier transform of the reconstructed density fluctuation spectrum was used to obtain the two-point cross-correlation function in excellent agreement with the initial one (see Fig.3).

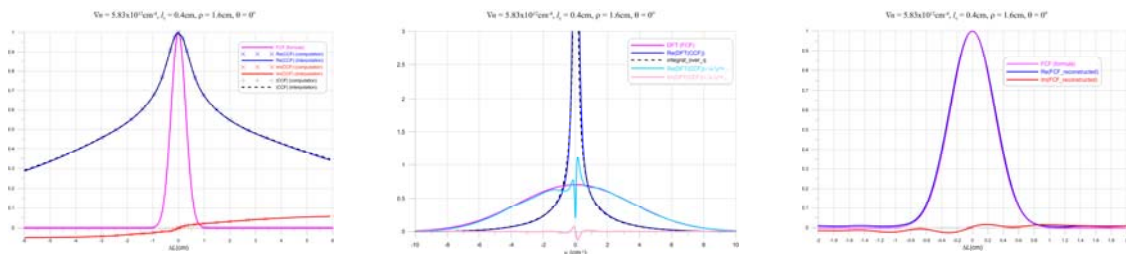


Fig.1 The RCR CCF.  
Blue - real part, red - imaginary part, black – absolute value, magenta - the turbulence CCF

Fig.2 The RCR and turbulence radial wavenumber spectra. Blue – RCR (real part); magenta – turbulence; light blue and rose – reconstructed real and imaginary parts.

Fig.3 The reconstructed turbulence CCF. Blue and red – real and imaginary parts of reconstructed CCF; magenta – initial turbulence CCF

We applied the 1D reconstruction procedure to the case of slightly oblique ( $\theta = 10^\circ$ ) incidence of the probing wave as well. The same plasma parameters and the reflectometer frequency were used in the computations. As it is seen in Fig.4, the width of the RCR CCF decreases in this case due partial suppression of small-angle scattering predicted in [3], remaining, however, still much larger than the turbulence correlation length. Nevertheless,

utilization of this CCF in the 1D reconstruction procedure [1] based on equation (1) leads to the turbulence spectrum which is similar to the Gaussian spectrum of turbulence (see Fig.5). Finally, the reconstructed turbulence two-point CCF is also obtained in Fig.6 in agreement with the computation input. However, they differ at large separation of the points  $\Delta L$ , and the imaginary part of the reconstructed turbulence CCF is larger here than in the normal incidence case.

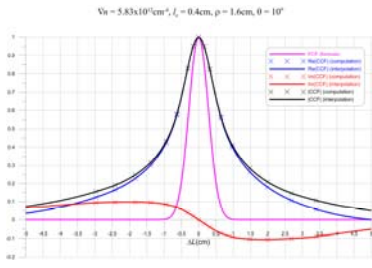


Fig.4 The RCR CCF.  
Blue - real part, red - imaginary part, black – absolute value, magenta - the turbulence CCF.  
 $\theta = 10^\circ$

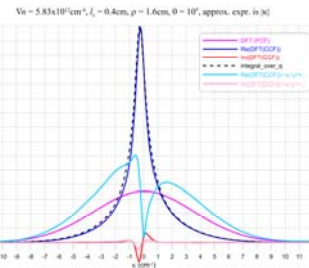


Fig.5 The RCR and turbulence radial wavenumber spectra. Blue – RCR (real part); magenta – turbulence; light blue and rose – reconstructed real and imaginary parts.  $\theta = 10^\circ$

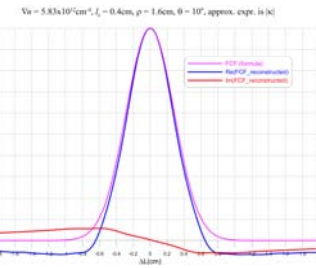


Fig.6 The reconstructed turbulence CCF. Blue and red – real and imaginary parts of reconstructed CCF; magenta – initial turbulence CCF.  $\theta = 10^\circ$

We have also confirmed the feasibility of the 1D procedure in the case of the normal incidence of a narrower probing beam ( $\rho = 0.8cm$ ), for which the cutoff is already situated in the antenna wave field. The corresponding spectra and CCFs are shown in Fig.7–9.

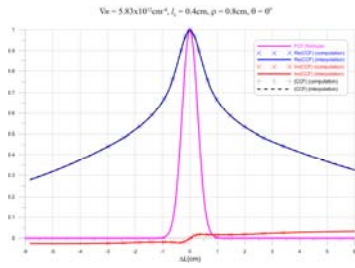


Fig.7 The RCR CCF. Blue - real part, red - imaginary part, black – absolute value, magenta - the turbulence CCF.

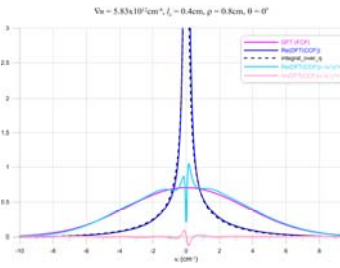


Fig.8 The RCR and turbulence radial wavenumber spectra. Blue – RCR (real part); magenta – turbulence; light blue and rose – reconstructed real and imaginary parts.

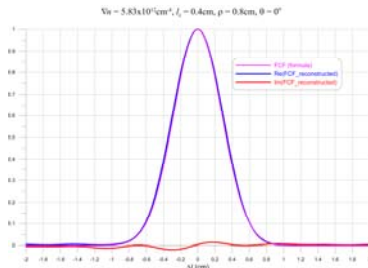


Fig.9 The reconstructed turbulence CCF. Blue and red – real and imaginary parts of reconstructed CCF; magenta – initial turbulence CCF.

Summarizing, we would like to underline that the turbulence spectrum reconstruction procedure from the RCR data proposed in [1] based on the 1D theory predictions appears to be very effective when applied to the interpretation of the realistic 2D computational data and thus could be recommended for implementation at fusion reflectometry experiments.

*Partial financial supports of RFBR grant 12-02-00515, NWO-RFBR Centre of Excellence on Fusion Physics and Technology (grant 047.018.002) and the Russian Academy Presidium program 12 are acknowledged.*

- [1] E. Z. Gusakov, N. V. Kosolapova Plasma Phys. Control. Fusion **53** (2011) 045012
- [2] N Teplova (Kosolapova), K Itoh, S-I Itoh et al. Phys. Scr. **87** (2013) 045502
- [3] E Gusakov, M Irzak and A Popov Plasma Phys. Control. Fusion **56** (2014) 025009